

DISCOVERY OF THE MOST ISOLATED GLOBULAR CLUSTER IN THE LOCAL UNIVERSE

IN SUNG JANG, SUNGSOON LIM, HONG SOO PARK, AND MYUNG GYOON LEE

Astronomy Program, Department of Physics and Astronomy, Seoul National University, Gwanak-gu, Seoul 151-742, Republic of Korea
Draft version March 6, 2018

ABSTRACT

We report the discovery of two new globular clusters in the remote halos of M81 and M82 in the M81 Group based on the Hubble Space Telescope archive images. They are brighter than typical globular clusters ($M_V = -9.34$ mag for GC-1 and $M_V = -10.51$ mag for GC-2), and much larger than known globular clusters with similar luminosity in the Milky Way Galaxy and M81. Radial surface brightness profiles for GC-1 and GC-2 do not show any feature for tidal truncation in the outer part. They are located much farther from either of M81 and M82 in the sky, compared with previously known star clusters in these galaxies. Color-magnitude diagrams of resolved stars in each cluster show a well-defined red giant branch (RGB), indicating that they are metal-poor and old. We derive a low metallicity with $[\text{Fe}/\text{H}] \approx -2.3$ and an old age ~ 14 Gyr for GC-2 from the analysis of the absorption lines in its spectrum in the Sloan Digital Sky Survey in comparison with the simple stellar population models. The I -band magnitude of the tip of the RGB for GC-2 is 0.26 mag fainter than that for the halo stars in the same field, showing that GC-2 is ~ 400 kpc behind the M81 halo along our line of sight. The deprojected distance to GC-2 from M81 is much larger than any other known globular clusters in the local universe. This shows that GC-2 is the most isolated globular cluster in the local universe.

Subject headings: galaxies: evolution — galaxies: individual (M81, M82) — galaxies: star clusters: general — galaxies: groups: individual (M81 Group)

1. INTRODUCTION

According to the current paradigm of large scale structure formation, individual galaxies, galaxy clusters, and groups are formed via hierarchical merging of galaxies. Globular clusters are a powerful tool to test this hypothesis. Globular clusters are often found in and around galaxies. With the advent of wide field surveys, globular clusters are sometimes found in the remote halo of galaxies in the Local Group. A small number of globular clusters are found beyond 30 kpc from the center of the Milky Way Galaxy (MWG) and M31 (Harris 1996; Huxor et al. 2008; Galleti et al. 2007), while most of the globular clusters are much closer to the galaxy center. A few clusters are found also in the remote halo of less massive galaxies such as NGC 6822 (Hwang et al. 2011) and M33 (Stonkutė et al. 2008; Cockcroft et al. 2011). Recently intracluster globular clusters are also found in nearby galaxy clusters: Virgo (Williams et al. 2007; Lee et al. 2010), Coma (Peng et al. 2011), and Abell 1835 (West et al. 2011). Globular clusters in galaxies provide fossil records for early formation of spheroidal components in the collapsing phase, while globular clusters far from galaxies reveal clues for later growth of galaxies via accretion.

The M81 Group, one of the nearest galaxy groups, is an excellent laboratory for studying the property of dwarf galaxies and star clusters as well as starburst galaxies and intergalactic medium (Chiboucas et al. 2009). The main galaxy located in the center of the group is M81, surrounded by 29 member galaxies (Chiboucas et al. 2009; Makarov & Karachentsev 2011). According to Makarov & Karachentsev (2011), the systemic velocity with respect to the Local Group and the velocity dis-

persion of the M81 Group are $v_{LG} = 193$ km s⁻¹ and $\sigma_v = 138$ km s⁻¹, respectively, and the total mass derived from the velocity of the members is $M = 3.89 \times 10^{12} M_\odot$. The M81 Group includes also a famous starburst galaxy M82. Karachentsev & Kashibadze (2006) estimate from kinematics and distances of the member galaxies that M81 is twice as massive as M82 and the mass of the M81 Group is 77% of the mass of the Local Group.

The distance to M81 is known to be 3.63 ± 0.14 Mpc ($((m-M)_0 = 27.80 \pm 0.08)$ derived using the tip of the red giant branch (TRGB) method from deep HST images as well as Cepheids by Durrell et al. (2010). The distance to M81 is estimated to be similar to that to M82 based on the same TRGB method, 3.55 ± 0.11 Mpc ($((m-M)_0 = 27.75 \pm 0.07)$) (Lee & Lim 2012), showing that these two galaxies are at a similar distance from us.

Previous studies found numerous star clusters in M81 and M82, which are mostly located in the main body of each galaxy (Mayya et al. 2008; Nantais et al. 2010; Nantais & Huchra 2010; Santiago-Cortés et al. 2010, 2011; Nantais et al. 2011). We have been searching for globular clusters in a remote halo region of each galaxy, much farther from previous surveys. In this paper we present a discovery of two globular clusters in the remote region of M81 and M82. This paper is composed as follows. In Section 2, we describe data used and the globular cluster search method. Section 3 presents the discovery of two new globular clusters, the color-magnitude diagrams of resolved stars in each cluster, and distance measurements. We also present the measurements of metallicity, age, and $[\alpha/\text{Fe}]$ using the spectrum of one globular cluster. Finally we derive the surface brightness profiles of the new globular clusters. Primary results are discussed and summarized in the final section.

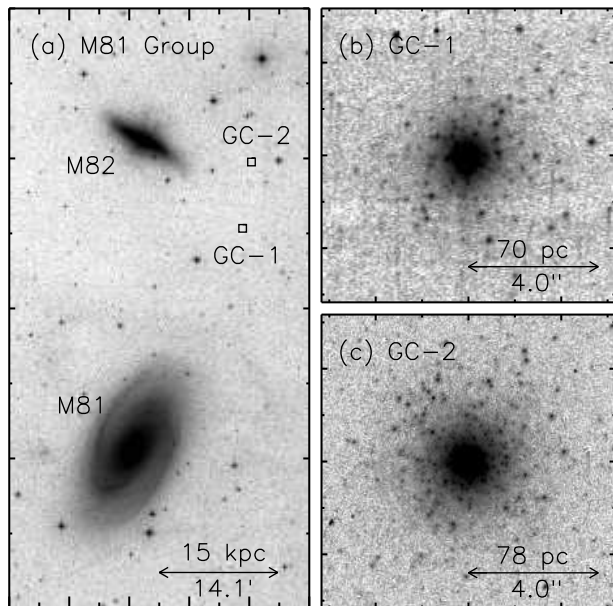


FIG. 1.— (a) A gray scale map of the digitized sky survey for the central region of the M81 Group, showing the positions of GC-1 and GC-2 discovered in this study. North is up and east to the left. (b) and (c) Gray scale maps of the $F814W$ images for GC-1 and GC-2.

2. DATA AND CLUSTER SEARCH

We used the images taken with the Hubble Space Telescope (HST)/Advanced Camera for Surveys (ACS) and Wide Field Camera 3 (WFC3) in the archive to search for globular clusters in the remote halo of M81 and M82. There are ~ 50 sets of multi-band images for the remote regions in the M81 group available. The images in which we found new globular clusters are ACS/WFC $F606W$ and $F814W$ images (obtained with exposure times 850 s and 690 s, respectively), and WFC3/UVIS $F606W$ and $F814W$ images (obtained with exposure times 735 s and 1225 s, respectively). Both fields come from the HST program 11613 (P.I. : de Jong).

We expected that globular clusters far from galaxies are more extended than those close to galaxy centers, so that some stars in the outer region of these globular clusters at the distance of the M81 Group can be resolved in the HST images. We searched all these fields visually with a primary aim to find globular clusters. To identify an object as a globular cluster, we used the following visual criteria : (1) round appearance, (2) lack of a smooth extended halo typical of background elliptical galaxies, and (3) being surrounded by an excess of resolved stars.

3. RESULTS

3.1. Discovery of New Globular Clusters

Through visual search we discovered two new globular clusters, JM81GC-1 and JM81GC-2 (called GC-1 and GC-2 hereafter), in ACS/WFC and WFC3/UVIS fields, respectively. Figure 1(a) shows the location of these globular clusters. GC-1 is $15'.90$ west of M82 and $29'.58$ north of M81 (corresponding projected distances are 17.07 kpc and 31.77 kpc, respectively). GC-2 is $13'.34$ west of M82 and $37'.25$ north of M81 (corresponding projected distances are 14.32 kpc and 40.00 kpc, respectively). Their positions are $RA(2000)=09^h 53^m 26.22^s$,

$Dec(2000)=69^\circ 31' 17''.5$ for GC-1, and $RA(2000)=09^h 53^m 20.17^s$, $Dec(2000)=69^\circ 39' 16''.4$ for GC-2.

We checked the images of these clusters in the Sloan Digital Sky Survey (SDSS) (York et al. 2000). GC-1 and GC-2 appear as extended source in the SDSS images and were classified as galaxies (SDSS ID : J095326+693117 for GC-1 and J095320+693916 for GC-2). However, $F814W$ images in Figure 1(b) and (c) show some resolved stars in the outer region of these clusters, proving that they are genuine star clusters. We checked the existence of any nearby dwarf galaxies around these two clusters using the data in Chiboucas et al. (2009) as well as the HST images, but found none.

3.2. Color-Magnitude Diagrams of Resolved Stars

We derived instrumental magnitudes of point sources in the images using the IRAF/ DAOPHOT package that is designed for point spread function (PSF) fitting photometry (Stetson 1994). We used $2\text{-}\sigma$ as the detection threshold, and derived the PSFs using isolated bright stars in the images. We applied aperture correction derived from isolated bright stars. We calibrated the instrumental magnitudes to the Vega magnitude system using photometric zeropoints for ACS/WFC (<http://www.stsci.edu/hst/acs/analysis/zeropoints/#tablestart>) and WFC3/UVIS (http://www.stsci.edu/hst/wfc3/phot_zp_lbn). Then we converted this system to Johnson-Cousins VI system using Sirianni et al. (2005).

Figures 2(a)–(d) display the color-magnitude diagrams for GC-1 and GC-2 as well as corresponding fields (called Field 1 and Field 2, respectively). Because the crowding is severe in the central region of the globular clusters, we plotted the stars at $0''.8 < r < 6''.0$ from the cluster center. The aperture with radius of $6''$ covers about 96 % of the total luminosity of each star cluster. In the case of fields, we plotted the stars at $15'' < r \lesssim 100''$. Both clusters show a relatively well-defined red giant branch (RGB), indicating that they may be old globular clusters.

3.3. Distance Estimation

We derived the distance to these clusters as well as to the corresponding halos using the TRGB method (Lee et al. 1993; Sakai et al. 1996; Méndez et al. 2002; McConnachie et al. 2004; Mouhcine et al. 2010; Conn et al. 2011). In Figure 2(e) the I -band luminosity function of the red giants in GC-1 and Field-1 shows a sudden jump at $I \approx 24.0$, which corresponds to the TRGB. However, the TRGB magnitude for GC-2 is about 0.3 mag fainter than that for Field-2 in Figure 2(g), showing that GC-2 may be behind the halo stars.

Using the edge-detecting algorithm, we determined the TRGB magnitude more quantitatively. We calculated an edge-detection response function $E(m) (= \Phi(m + \sigma_m) - \Phi(m - \sigma_m))$ where $\Phi(m)$ is the luminosity function of magnitude m and σ_m is the mean photometric error within a bin of ± 0.05 mag about magnitude m , and we weighted it according to the Poisson noise of the luminosity function $E(m) \sqrt{\Phi(m)}$ (Méndez et al. 2002), as shown in Figures 2(f) and (h).

Thus derived TRGB magnitudes are $I_{TRGB} = 24.039 \pm 0.021$ for GC-1, 24.069 ± 0.011 for Field-1, 24.295 ± 0.036

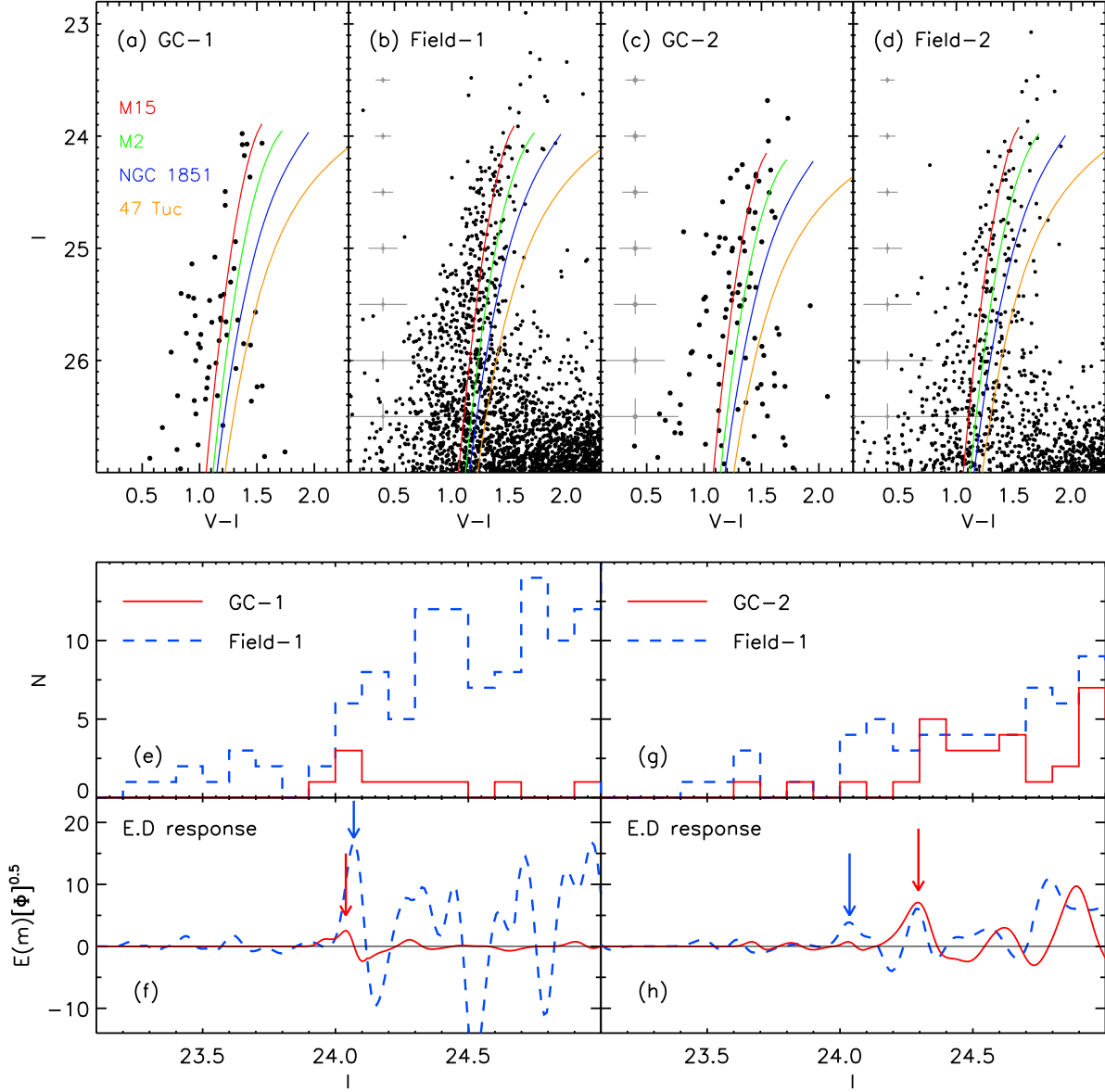


FIG. 2.— (a)–(d) I - $(V-I)$ color-magnitude diagrams of the stars in the region at $0''.8 < r < 6''.0$ for GC-1 and GC-2 and in their corresponding fields at $15'' < r \lesssim 100''$. The curved lines represent the loci of the RGB in the Milky Way globular clusters with a range of metallicity ($[\text{Fe}/\text{H}] = -2.17, -1.58, -1.29, \text{ and } -0.71$, respectively), shifted according to the foreground reddening and derived distance. Errorbars represent the mean errors. (e)–(h) I -band luminosity functions of red giants with $0.7 < (V-I) < 1.9$ (e and g), and weighted edge-detection responses (f and h). Arrows represent the positions of the TRGB.

for GC-2, and 24.036 ± 0.022 for Field-2. The errors for the TRGB magnitudes were determined using bootstrap resampling method with one million simulations. In each simulation, we resampled randomly the RGB sample with replacement to make a new sample of the same size. We estimated the TRGB magnitude for each simulation using the same procedure and derived the standard deviation of the estimated TRGB magnitudes.

The mean color of the TRGB is derived from the colors of the bright red giants close to the TRGB and is corrected for the foreground reddening ($E(B-V) = 0.09$ for GC-1 and $E(B-V) = 0.10$ for GC-2 (Schlegel et al. 1998)): $(V-I)_{0,\text{TRGB}} = 1.32 \pm 0.02$ for GC-1, 1.41 ± 0.03 for Field-1, 1.31 ± 0.04 for GC-2, and 1.49 ± 0.04 for Field-2. We derive the intrinsic I -band magnitude of the

TRGB using the relation between the bolometric magnitude M_{bol} and the bolometric correction BC : $M_{I_0} = M_{\text{bol}} - BC_{I_0}$. We calculate the bolometric magnitude using $M_{\text{bol}} = -0.19[\text{Fe}/\text{H}] - 3.81$ and the bolometric correction using $BC_{I_0} = 0.881 - 0.243(V-I)_{0,\text{TRGB}}$ (Da Costa & Armandroff 1990). $[\text{Fe}/\text{H}]$ is derived from the mean color of the RGB stars.

The mean color of the RGB stars 0.5 mag fainter than the TRGB is derived from the colors of the bright red giants close to this magnitude: $(V-I)_{0,-3.5} = 1.21 \pm 0.02$ for GC-1, 1.22 ± 0.03 for Field-1, 1.21 ± 0.03 for GC-2, and 1.31 ± 0.02 for Field-2. From these we derive $[\text{Fe}/\text{H}]$: $[\text{Fe}/\text{H}] = -2.23 \pm 0.11$ for GC-1, -2.18 ± 0.13 for Field-1, -2.23 ± 0.12 for GC-2, and -1.84 ± 0.10 for Field-2. Using these we obtain $M_{I,\text{TRGB}} = -3.95$ for GC-1, -3.93

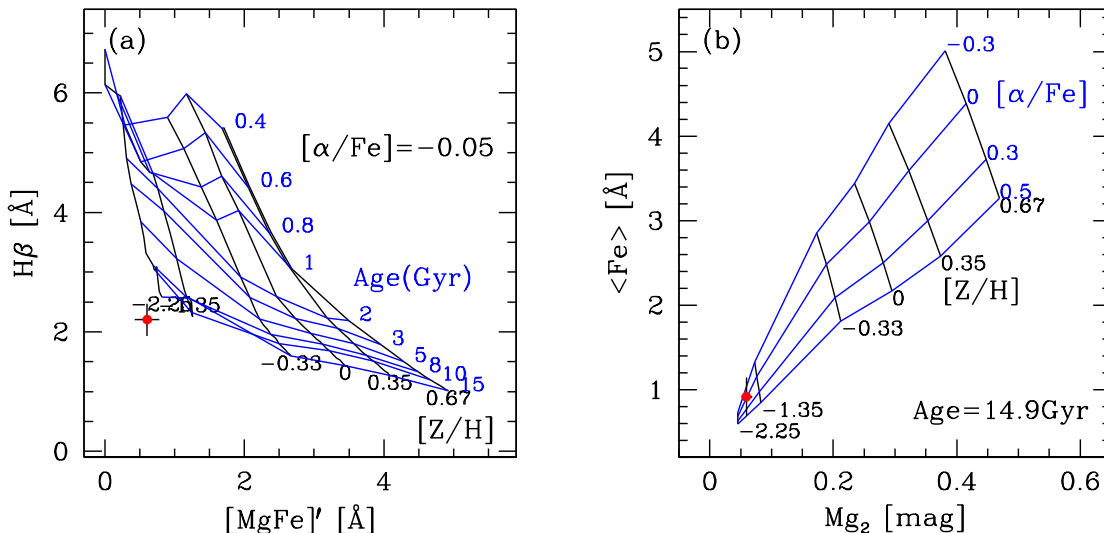


FIG. 3.— (a) Lick line indices for $H\beta$ versus $[MgFe]'$ for GC-2, useful for measuring the metallicity and age (dots with errorbars). Grids represent the SSP models for various values of $[Z/H]$ and age[Gyr] at $[\alpha/Fe] = -0.05$ given by Thomas et al. (2003). (b) $\langle Fe \rangle$ versus Mg_2 useful for measuring $[\alpha/Fe]$. The grids are for an age 14.9 Gyr.

for Field-1, -3.95 for GC-2, and -3.98 for Field-2. Thus we finally calculate the distance modulus using $(m - M)_0 = I_{0,TRGB} - M_{I,TRGB}$. The distances derived are $(m - M)_0 = 27.80 \pm 0.03$ ($d = 3.63 \pm 0.05$ Mpc) for GC-1, 27.81 ± 0.03 ($d = 3.65 \pm 0.05$ Mpc) for Field-1, 28.04 ± 0.04 ($d = 4.05 \pm 0.08$ Mpc) for GC-2, and 27.81 ± 0.03 ($d = 3.65 \pm 0.05$ Mpc) for Field-2. This value is similar to the previous estimates for M81, 3.63 ± 0.14 Mpc (Durrell et al. 2010; Gerke et al. 2011) and M82, 3.55 ± 0.11 Mpc (Lee & Lim 2012). While GC-1 is at the same distance as M81, GC-2 is about 400 kpc behind the M81 halo along our line of sight.

3.4. Spectral Line Analysis for GC-2

GC-2 was previously observed and classified as a galaxy in the SDSS and its optical spectrum is available in the SDSS. The spectrum of GC-2 shows several absorption lines typical for globular clusters. We derived $[Fe/H]$, $[\alpha/Fe]$, and age for GC-2 from the comparison of Lick line index diagrams with the simple stellar population (SSP) models by Thomas et al. (2003).

Figure 3 displays $H\beta$ versus $[MgFe]'$ diagram, and $\langle Fe \rangle$ versus Mg_2 diagram for GC-2. The composite index $[MgFe]'$ is a combination of magnesium and iron-sensitive indices, defined as $[MgFe]' = \sqrt{Mgb(0.72 \cdot Fe5270 + 0.28 \cdot Fe5335)}$. It is an excellent metallicity indicator, because it is completely independent of $[\alpha/Fe]$, and this behavior is almost independent of the adopted age or metallicity (Thomas et al. 2003). $H\beta$ is an efficient indicator for age. We used the line index data for these clusters provided by the SDSS. The values derived following the technique described in Puzia et al. (2005) and Park, Lee, & Hwang (2012) are $[Fe/H] = -2.3 \pm 0.12$, $[\alpha/Fe] = -0.05 \pm 0.40$, and age = 14.9 ± 1.0 Gyr. This metallicity is consistent with the value derived from the color of the RGB. These show that GC-2 is indeed very metal-poor and old.

3.5. Spectral Energy Distribution Fit

We also derived age and mass from the spectral energy distribution fit using SDSS *ugriz* magnitudes in com-

parison with the SSP model given by Bruzual & Charlot (2003) ($u = 20.50 \pm 0.12$, $g = 19.13 \pm 0.02$, $r = 18.50 \pm 0.02$, $i = 18.21 \pm 0.02$, and $z = 18.03 \pm 0.05$ for GC-1, and $u = 19.51 \pm 0.06$, $g = 18.25 \pm 0.01$, $r = 17.60 \pm 0.01$, $i = 17.31 \pm 0.01$, and $z = 17.10 \pm 0.03$ for GC-2). Derived ages are $\log(\text{age}[y]) \sim 10.2$ for both clusters as long as we adopt $Z = 0.0001$, and derived cluster masses are $\log(M/M_\odot) \sim 6.40$ for GC-1, and 6.85 for GC-2. This age for GC-2 is also consistent with the value derived from the spectrum analysis. Thus these clusters are very massive and old.

3.6. Surface Photometry

We derived surface photometry of GC-1 and GC-2 using IRAF/ELLIPSE task from the HST images. Figure 4 displays the radial profiles of the surface brightness for *F814W* images. The radial profiles of the inner region look similar to the King profiles. However, the outer parts in the radial profiles do not show any tidal cut-off, but continue to decrease smoothly. From the King model fits for the inner region at $0''.0 < r < 4''.0$, we derived core radii (r_c), $0''.0755 \pm 0''.0003$ (1.329 ± 0.005 pc) for GC-1 and $0''.1269 \pm 0''.0003$ (2.491 ± 0.006 pc) for GC-2. Also we fit the data using the model with a power law form in the outer region in Elson et al. (1987),

$$\sum(r_p) = \sum_0 \left(1 + \frac{r_p^2}{a^2}\right)^{-\gamma/2}$$

where the scale radius a is related with the King core radius as $r_c = a\sqrt{2^{2/\gamma} - 1}$ for $r_t \gg r_c$. There is a break at $r = 2''.80$ (55 pc) for GC-2 so that we fit the data in two parts: $a = 1.96$, $\gamma = 2.48$ for GC-1, and $a = 3.16$, $\gamma = 2.42$, $a = 3.27$, $\gamma = 3.62$ for GC-2. The radial surface brightness profiles of GC-1 and GC-2 gradually decrease out to $r = 15''$. By integrating the radial surface brightness profiles to $r = 15''$, we derived integrated magnitudes of the star clusters, which we shall present in Section 4.1. From these we derived half light radii (r_h): $0''.352 \pm 0''.006$ (6.13 ± 0.01 pc) for GC-1 and $0''.511 \pm 0''.005$ (9.81 ± 0.01 pc) for GC-2.

4. DISCUSSION AND SUMMARY

4.1. Luminosity-Size Relation

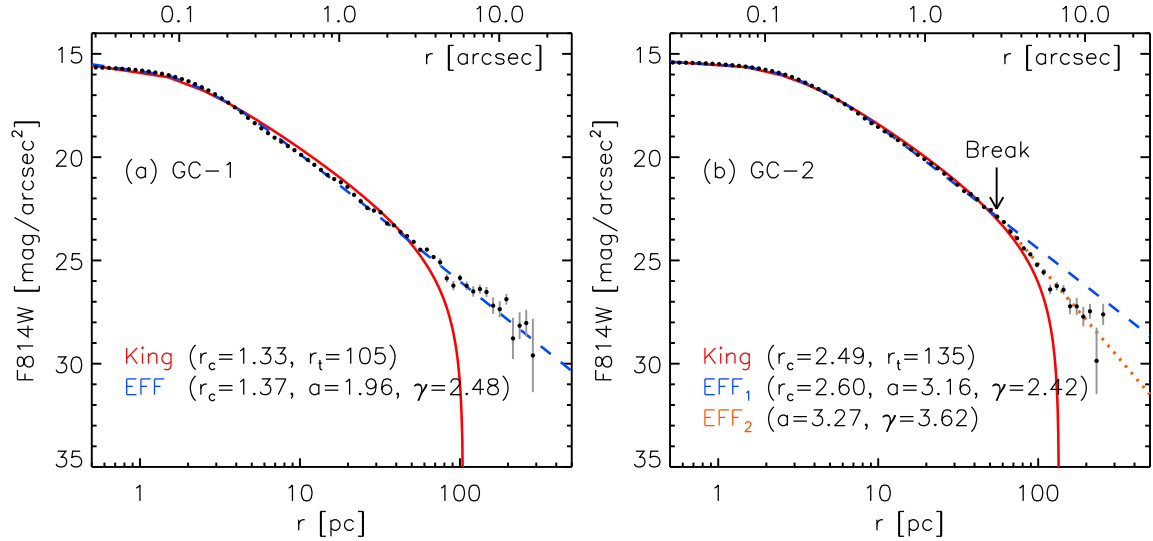


FIG. 4.— $F814W$ -band surface brightness profiles for GC-1 (a) and GC-2 (b) (dots with errorbars). The thick solid lines represent the King model fit and the dotted and dashed lines represent the EFF power-law model fit.

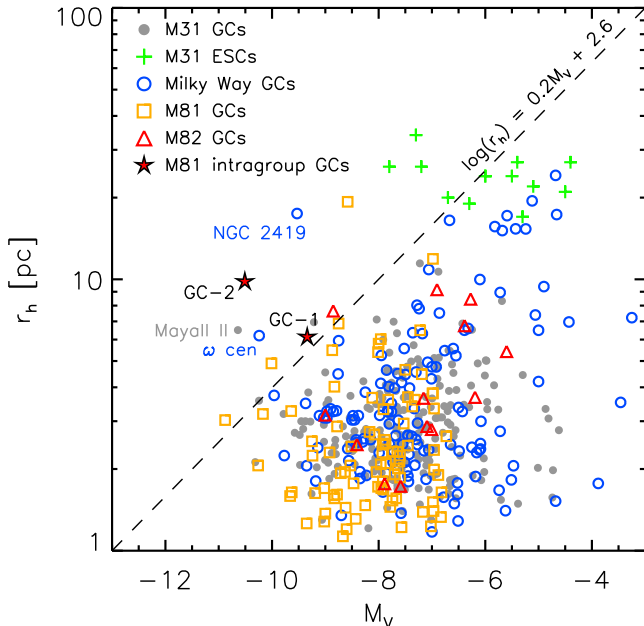


FIG. 5.— Half light radii (r_h [pc]) versus M_V for GC-1 and GC-2 (star symbols) in comparison with globular clusters in the Milky Way Galaxy (open circles) (Harris 1996), M31 (filled circles and crosses) (Huxor et al. 2009, 2011), M81 (open squares) (Nantais et al. 2010, 2011), and M82 (open triangles) (Lim, Hwang, & Lee 2012).

Integrated magnitudes and colors of GC-1 and GC-2 are derived, respectively, $V_0 = 18.46 \pm 0.01$ and $(V - I)_0 = 0.91 \pm 0.01$ and $V_0 = 17.53 \pm 0.01$ and $(V - I)_0 = 0.90 \pm 0.01$. Corresponding absolute magnitudes are $M_V = -9.34 \pm 0.01$ for GC-1 and -10.51 ± 0.01 for GC-2, derived using our TRGB distances to the clusters. In Figure 5 we plot half light radii (r_h) versus absolute magnitude M_V for GC-1 and GC-2 in comparison with globular clusters in the Milky Way Galaxy (Harris 1996), M81 (Nantais et al. 2011) and M82 (Lim, Hwang, & Lee 2012). We also plotted the

data for globular clusters and extended star clusters in M31 (Huxor et al. 2009, 2011).

van den Bergh & Mackey (2004) presented a boundary relation between normal globular clusters and extended globular clusters: $\log(r_h) = 0.2M_V + 2.6$. GC-1 and GC-2 are found to be located above this boundary line, like the case of ω Cen and NGC 2419 in our Galaxy, and Mayall II in M31. Thus GC-1 and GC-2 are larger than typical globular clusters with similar luminosity, and they are much brighter than the extended star clusters in M31. The latter globular clusters (ω Cen, NGC 2419, and Mayall II) show some peculiar features so that they are often considered to be remnants of dwarf galaxies. Therefore GC-1 and GC-2 also may be in the same vein.

4.2. Intragroup Globular Clusters

At the moment the most isolated globular cluster in the Local Group is known to be MGC1, located at the projected distance from M31, 117 kpc. Considering it is ~ 160 kpc closer than M31, its deprojected distance from M31 was derived to be 200 ± 20 kpc (Mackey et al. 2010). It is brighter ($M_V = -9.2$) than typical globular clusters, but fainter than GC-1 in M81. In the Milky Way Galaxy, the most distant globular clusters and their galactocentric distances are NGC 2419 (91.5 kpc), Pal 3 (95.9 kpc), Eridanus (95.2 kpc), Pal 4 (111.8 kpc), and AM-1 (123.2 kpc) (Harris 1996).

On the other hand the most distant satellite dwarf galaxies in the two main Local Group galaxies are Leo I in the Milky Way Galaxy and And XXVIII at $d > 350$ kpc in M31 (Slater et al. 2011). Leo I is a dwarf spheroidal galaxy located at 270 kpc, being considered long as the most distant satellite of the Milky Way Galaxy (Lee et al. 1993). And XXVIII is a newly discovered dwarf galaxy about 100 kpc closer than M31. Its deprojected distance from M31 is estimated to be 365_{-1}^{+17} kpc (Slater et al. 2011). Thus the most remote globular clusters in our Galaxy and M31 are closer than the most distant satellite dwarf galaxies. This raises interesting questions: *Can there be any globular clusters more dis-*

tant than the most distant satellite galaxies in a galaxy? If so, what are they?

GC-2 lies 406 ± 97 kpc behind M81 along our line of sight, according to our TRGB distance estimates to GC-2 and Field-2. Considering this and the projected distance in the sky we derive a three-dimensional distance from M81, 408 ± 97 kpc. Although it is closer to M82 than M81 in the sky, its three dimension distance is significantly larger than the projected distance from M82 (also from M81). Also M81 is twice as massive as M82 and is the most massive member in the M81 Group. These indicate that the main host for GC-2 may be, if any, M81 rather than M82. Therefore GC-2 is the most isolated globular cluster among the known globular clusters in the local universe. In addition, it is more distant than any known satellite dwarf galaxies around M81. The radial velocity for GC-2 given in the SDSS is 159 ± 4 km s⁻¹, which is much larger than the value for M81 (-35 ± 4 km s⁻¹) (Chynoweth et al. 2008). Thus GC-2 is receding with a velocity ≈ 200 km s⁻¹ from M81. If this were moving at this velocity along the radial orbit, it would have taken about 2 Gyr to reach the current position from the center of M81. Thus GC-2 can be considered as an intragroup

globular cluster wandering in the M81 Group.

How can GC-2 be that far from M81, receding with a velocity of ≈ 200 km s⁻¹? The origin of GC-2 is not clear. Possible scenarios are as follows. First, it might have ejected during the interaction of three main galaxies about 2 Gyr ago. However, there are no evidence supporting this at the moment. Second, it may be one of the primordial globular clusters that formed early in isolation. If so, where are others? Third, it may a remnant of a dwarf galaxy that accreted to M81 and is receding now. If so, how could it survive during the perigalactic passage around M81? These possibilities need to be investigated with observations or simulations.

The authors thank anonymous referee for useful suggestions. M.G.L. was supported in part by Mid-career Research Program through the NRF grant funded by the MEST (no.2010-0013875). I.S.J. and S.L. are grateful to Yeong Su Kim for financial support through the In Ha Kim scholarship. This paper is based on image data that obtained from Multimission Archive at the Space Telescope Science Institute (MAST).

REFERENCES

- Bruzual, G., & Charlot, S. 2003, MNRAS, 344, 1000
 Chiboucas, K., Karachentsev, I. D., & Tully, R. B. 2009, AJ, 137, 3009
 Chynoweth, K. M., Langston, G. I., Yun, M. S., et al. 2008, AJ, 135, 1983
 Cockcroft, R., Harris, W. E., Ferguson, A. M. N., et al. 2011, ApJ, 730, 112
 Conn, A. R., Lewis, G. F., Ibata, R. A., et al. 2011, ApJ, 740, 69
 Da Costa, G. S., & Armandroff, T. E. 1990, AJ, 100, 162
 Durrell, P. R., Sarajedini, A., & Chandar, R. 2010, ApJ, 718, 1118
 Elson, R. A. W., Fall, S. M., & Freeman, K. C. 1987, ApJ, 323, 54
 Gerke, J. R., Kochanek, C. S., Prieto, J. L., et al. 2011, ApJ, 743, 176
 Galletti, S., Bellazzini, M., Federici, L., et al. 2007, A&A, 471, 127
 Harris, W. E. 1996, AJ, 112, 1487
 Huxor, A. P., Tanvir, N. R., Ferguson, A. M. N., et al. 2008, MNRAS, 385, 1989
 Huxor, A., Ferguson, A. M. N., Barker, M. K., et al. 2009, ApJ, 698, L77
 Huxor, A. P., Ferguson, A. M. N., Tanvir, N. R., et al. 2011, MNRAS, 414, 770
 Hwang, N., Lee, M. G., Lee, J. C., et al. 2011, ApJ, 738, 58
 Karachentsev, I. D., & Kashibadze, O. G. 2006, Astrophysics, 49, 3
 Lee, M. G., Freedman, W. L., & Madore, B. F. 1993, ApJ, 417, 553
 Lee, M. G., Freedman, W. L., Mateo, M., et al. 1993, AJ, 106, 1420
 Lee, M. G., Park, H. S., & Hwang, H. S. 2010, Science, 328, 334
 Lee, M. G., & Lim, S. 2012, in preparation
 Lim, S., Hwang, N., & Lee, M. G. 2012, in preparation
 McConnachie, A. W., Irwin, M. J., Ferguson, A. M. N., et al. 2004, MNRAS, 350, 243
 Mackey, A. D., Ferguson, A. M. N., Irwin, M. J., et al. 2010, MNRAS, 401, 533
 Makarov, D., & Karachentsev, I. 2011, MNRAS, 412, 2498
 Mayya, Y. D., Romano, R., Rodríguez-Merino, L. H., et al. 2008, ApJ, 679, 404
 Méndez, B., Davis, M., Moustakas, J., et al. 2002, AJ, 124, 213
 Mouhcine, M., Harris, W. E., Ibata, R., et al. 2010, MNRAS, 404, 1157
 Nantais, J. B., Huchra, J. P., McLeod, B., et al. 2010, AJ, 139, 1413
 Nantais, J. B., & Huchra, J. P. 2010, AJ, 139, 2620
 Nantais, J. B., Huchra, J. P., Zezas, A., et al. 2011, AJ, 142, 183
 Park, H. S., Lee, M. G., & Hwang, H. S. 2012, ApJ, submitted
 Peng, E. W., Ferguson, H. C., Goudfrooij, P., et al. 2011, ApJ, 730, 23
 Puzia, T. H., Perrett, K. M., & Bridges, T. J. 2005, A&A, 434, 909
 Sakai, S., Madore, B. F., & Freedman, W. L. 1996, ApJ, 461, 713
 Santiago-Cortés, M., Mayya, Y. D., & Rosa-González, D. 2010, MNRAS, 405, 1293
 Santiago-Cortés, M., Mayya, Y. D., & Rosa-González, D. 2011, Revista Mexicana de Astronomía y Astrofísica Conference Series, 40, 94
 Schlegel, D. J., Finkbeiner, D. P., & Davis, M. 1998, ApJ, 500, 525
 Sirianni, M., Jee, M. J., Benítez, N., et al. 2005, PASP, 117, 1049
 Slater, C. T., Bell, E. F., & Martin, N. F. 2011, ApJ, 742, L14
 Stetson, P. B. 1994, PASP, 106, 250
 Stokutė, R., Vansevicius, V., Arimoto, N., et al. 2008, AJ, 135, 1482
 Thomas, D., Maraston, C., & Bender, R. 2003, MNRAS, 339, 997
 van den Bergh, S., & Mackey, A. D. 2004, MNRAS, 354, 713
 West, M. J., Jordán, A., Blakeslee, J. P., et al. 2011, A&A, 528, A115
 Williams, B. F., Ciardullo, R., Durrell, P. R., et al. 2007, ApJ, 654, 835
 York, D. G., Adelman, J., Anderson, J. E., Jr., et al. 2000, AJ, 120, 1579